Periodontal regeneration induced by porous alpha-tricalcium phosphate with immobilized basic fibroblast growth factor in a canine model of 2-wall periodontal defects

Kazuya Matsuse[1], Yoshiya Hashimoto [2,*], Sachiro Kakinoki [3],Tetsuji Yamaoka [3] and Shosuke Morita[1]

[1] First Department of Oral and Maxillofacial Surgery, Osaka Dental University

[2] Department of Biomaterials, Osaka Dental University

[3] Department of Biomedical Engineering, National Cerebral and Cardiovascular Center Research Institute

Medical morecular morphology. Volume 51, Number 1, pp48-56 掲載

Abstract:

We evaluated the effect of porous alpha-tricalcium phosphate (α-TCP) with immobilized basic fibroblast growth factor (bFGF) on periodontal regeneration in a canine model of 2-wall periodontal defects. Identical bone defects were made in the canine mandible; six defects in each animal were filled with porous α-TCP with bFGF bound via heparin (bFGF group), and the remaining defects were filled with unmodified porous α-TCP (control group). Micro-computed tomography and histological evaluation were performed at 2, 4, and 8 weeks post-implantation. The bone mineral content of the bFGF group was higher than that of the control group at 2 and 4 weeks ($p < 0.05$). Histological evaluation at 2 weeks post-implantation revealed degradation of the porous α-TCP, and bone had formed on the surface of α-TCP particles in the bFGF group. Some of these collagen fibers connected the newly formed cementum with the alveolar bone, revealing the formation of new periodontal ligaments with Sharpey's fibers. At 8 weeks, continuous cortical bone with a Haversian structure covered the top of the bone defects in the bFGF group. These findings indicate that porous α-TCP with

immobilized bFGF could promote periodontal regeneration at the early regeneration phase in a canine model of 2-wall periodontal defects.

Introduction

Regeneration of periodontal tissue is the ultimate goal of periodontal therapy. However, no conventional periodontal or surgical treatment developed thus far can functionally regenerate lost periodontal tissue. To address this limitation, various new regenerative therapies, such as those involving scaffold implantation [1,2], differentiation of stem cells [3], and application of an enamel matrix derivative [4], have been introduced to periodontal surgeries and have resulted in a periodontal regenerative effect.

Several bone-grafting materials are commonly used in periodontal regenerative therapy, either alone or together with other materials as scaffolds. Hydroxyapatite and tricalcium phosphate (TCP) implants are well known to possess high tissue compatibility; moreover, new bone can form directly on these implants [1,5]. Alpha (α-)TCP is thermodynamically stable at temperatures above 1100°C and shows higher degradability than β-TCP [6]. Porous TCP also has potential for application as a space-making material and a drug delivery system in bone defects [6].

Basic fibroblast growth factor (bFGF) regulates bone formation and remodeling [7]; however, it is highly unstable in physiological environments. As such, its activity is rapidly reduced after implantation into the body. Recently, we showed that specific binding of bFGF to heparin and subsequent tissue integration was accelerated by immobilizing bFGF on porous polymeric materials in a mild and biologically safe reaction [8]. In addition, we successfully immobilized bFGF on porous α-TCP using heparin and evaluated the ability of this bFGF carrier to induce bone formation and remodeling in the early stages of recovery (2 weeks after surgery) in a canine mandibular bone defect model [9].

Large circumferential periodontal defects without bony walls are considered difficult to treat because it may not be possible to maintain the blood clot to promote healing or to preserve space for periodontal tissue regeneration [10]. The combination of growth/differentiation factors and scaffolds

could enhance periodontal regeneration in different critically sized defects in animals [11-13]. Biodegradable devices for the treatment of periodontal bone defects, consisting of a combination of recombinant human platelet-derived growth factor BB (rhPDGF-BB) and β-TCP matrix, are currently either on the market or being developed [14]. The first product in this class, GEM 21STM (Luitpold Pharmaceuticals, Shirley, NY, USA), contains β-TCP particles and has been approved by the United States Food and Drug Administration [14]. However, rhPDGF-BB is not chemically adsorbed on the particle surface and is more likely to be physically entrapped between and within hydrated particles. Therefore, a carrier/delivery system is necessary for binding of growth factors such as bFGF. In this study, we aimed to immobilize bFGF on porous α-TCP using heparin and then evaluate the effect of this bFGF carrier on periodontal regeneration in a canine model of 2-wall periodontal defects.

Materials and Methods

Materials

Porous α-TCP particles with an average diameter of 580 μm and porosity of approximately 80% were obtained from Taihei Chemical Industrial Co. (Osaka, Japan) and sterilized by dry heating before the experiment. The surface-modifier peptide was purchased from SCRUM (Tokyo, Japan). Distilled water and 1000 units/mL heparin solution were supplied by Mochida Pharmaceutical Co. (Tokyo, Japan). bFGF (KCB-1 and Fiblast Spray) was obtained from Kaken Pharmaceutical Co. (Osaka, Japan).

Surface Modification of α-TCP Particles

A predetermined amount of α-TCP particles was added to 0.1% peptide solution in distilled water (1:3 w/v) and incubated for 24 h at 50°C in the dark. After rinsing three times with three volumes of distilled water, the particles were dried overnight and then immersed in heparin solution (1:3 w/v) for 8 h at 37°C, followed by three rinses as described above and overnight drying in a vacuum. bFGF was immobilized on the heparin-modified α-TCP particles by immersing the particles in 1 mg/mL bFGF (Fiblast Spray; Kaken Pharmaceutical Co.) in distilled water (1:3 w/v) for 24 h at 4°C, followed by three rinses with distilled water. The procedure was performed in a sterile environment.

Surface Analysis

The surface morphology and elemental composition of the α-TCP particles were evaluated by scanning electron microscopy (SEM) (JSM-5700; JEOL, Tokyo, Japan) and X-ray photoelectron spectroscopy (XPS) (ESCA-3400; Shimadzu, Kyoto, Japan), respectively.

Canine Mandibular Defect Model

The mandibular defect model was established using six healthy beagles (2 years old, weighing approximately 10 kg) that were obtained from Hamaguchi Animal (Osaka, Japan). The animals were housed in a temperature-controlled environment at 24°C with free access to food and water. The body weight and general health of the animals was monitored throughout the study. All procedures in this study were approved by the Animal Experiment Committee of Osaka Dental University and conformed to the guidelines described in the Guiding Principles for the Use of Laboratory Animals (approval Nos. 16-05002 and 17-05004).

The first and third premolars were extracted to create space for identical defects 2 months before treatment. An initial incision was made to the squamous epithelium of the gingiva that covered an appropriate part of the mandible, and the submucosal tissue was separated from the periosteum. A second incision was made in the periosteum of the mandible, which was lifted and carefully dissected from the underlying mandible. 2-wall periodontal defects (mesiodistal width: 5 mm × depth: 6 mm; buccolingual width: 4 mm) were surgically created on the mesial and distalbuccal portions of the mandibular second premolar and distalbuccal portion of the mandibular fourth premolar (Figure 1). Alveolar bone was removed using a steel bur and the root surfaces were planed with Gracey curettes to remove the cementum and PDL under general anesthesia (0.5 mg/kg pentobarbital sodium) and infiltration anesthesia (1.8 mL of 2% lidocaine hydrochloride and 1:80,000 epinephrine).

α-TCP Particle Implantation

The defects were then randomly filled with one of two treatments: bFGF bound to porous α-TCP via heparin, or unmodified porous α-TCP (control). The defects were assessed at 2, 4, and 8 weeks after surgery. The periosteum and skin overlying the defects were sutured in two layers with 3-

0 Vicryl (Ethicon GmbH & Co. KG, Norderstedt, Germany) and 3-0 MANI Silk (MANI, Tochigi, Japan). An anti-inflammatory agent, Carprofe (CarprodylVR; Ceva, Libourne, France), was administered daily for 7 days following each surgery (tooth extraction and implantation). Six defects per group were histologically analyzed at each follow-up time point.

Radiographical Analysis

Under general anesthesia, the canines were euthanized by exsanguination at 2, 4, and 8 weeks after surgery. The mandibles were harvested for examination by micro-computed tomography (SMX-130CT; Shimadzu, Kyoto, Japan). Blocks of bone specimen were mounted on the turntable. The exposure parameters were 51 kV and 120 mA. Data obtained from each slice were stored at a resolution of 512 × 512 pixels. TRI/3D BON software (version 7, Ratoc Co., Tokyo, Japan) was used to generate a 3D reconstruction using the volume-rendering method for morphological assessment. In the 3D analysis, the total volume (TV; cm^3), bone volume (BV; cm^3), and bone mineral content (BMC; mg) were measured using TRI/3D-BON software based on the obtained values. The volumetric density (VD) was then calculated according to the following formula: VD (%) = BV / TV.

Histological Assessment

The mandibles were fixed in 10% neutral-buffered formalin (Sigma, St. Louis, MO, USA), demineralized in a solution of ethylenediaminetetraacetic acid (Sigma), dehydrated in a graded series of alcohol, and embedded in paraffin. Fixed tissue samples were sectioned (5–7 μm thickness) in the coronal plane and stained with hematoxylin and eosin and Azan. For immunostaining to detect vascularization, deparaffinized rehydrated sections were treated with 0.1% trypsin, and vascular endothelial cells were labeled using a monoclonal anti-human von Willebrand (vW) Factor antibody at a final dilution of 1:1000 (Abcam, Cambridge, UK; ab6994). Immunoreactivity was detected using the EnVision system (Dako, Tokyo, Japan; K4003). Sections were visualized under a BZ9000 All-in-One Fluorescence Microscope (Keyence, Tokyo, Japan). New bone, cementum and periodontal ligament (PDL) formation were quantified by determining the new bone area (BA)/the total defect area (TA) (%), new cementum (NC)/total defect height (TH) (%), and new PDL (NP)/total defect

height (TA) (%) in each group, based on measurements from images 1 and 5 of Figures 5, 6, and 7, using ImageJ software (version 1.50i, National Institutes of Health, Bethesda, MD, USA), respectively.

Statistical Analysis

Data were evaluated by one-way analysis of variance followed by the Tukey–Kramer post-hoc test (OMS Publisher, Tokorozawa, Japan). Student's *t*-test was performed to compare the values of the bFGF and control groups at 2, 4, and 8 weeks. $p < 0.05$ was considered to indicate statistical significance.

Results

Analysis of Porous α-TCP Particles with Immobilized bFGF

The morphology and surface elements of the α-TCP particles before and after the reaction were analyzed by SEM and XPS, respectively. The synthesized α-TCP particles had a continuous pore structure, with a pore diameter of approximately 5–10 μm, as determined by SEM (Figure 2). A small sulfate peak (S2p) and a nitrogen peak (N1s), corresponding to heparin and bFGF, respectively, were detected by XPS analysis of bFGF bound to porous α-TCP via heparin (Figure 3 a, b).

3D Microradiography and Bone Mineral Density (BMD) Analysis

Quantitative imaging of the newly grown bone was performed by *in vivo* 3D microradiography using a BMD analysis system. The BMD, BMC, and VD of each group were determined at 2, 4, and 8 weeks (Figure 4). There were no significant differences in BMD and VD between the two groups at any time point ($p > 0.05$); however, the BMC of the bFGF group at 2 and 4 weeks was significantly higher than that of the control group ($p < 0.05$).

Histological Assessment

The newly formed and remodeled bones were subjected to histological analysis. Cross-sections of the bone defect sites obtained at 2, 4, and 8 weeks after surgery were stained with hematoxylin and eosin (Figure 5). At 2 weeks, more bone formation was observed in the bFGF group than in the control

group (Figure 5 a, d). In the bFGF group, α-TCP particles were encapsulated with normal connective tissue and degraded, and newly formed vessels were prominent around the surface of the α-TCP particles (Figure 5 b, c). Moreover, connective tissues with tightened collagen fibers were extended in the bFGF group (Figure 5 b), and some of these collagen fibers connected the new partially formed cementum with the alveolar bone, thus revealing the formation of new PDLs with Sharpey's fibers (Figure 5 d). In the control group, some of the α-TCP particles remained in their original form and newly formed vessels were observed in and around the surface of the α-TCP particles (Figure 5 f, g). The new connective tissue covered the root surface entirely.

At 4 weeks, most of the α-TCP particles in the bFGF group were degraded and replaced with new bone (Figure 6 b); however, new vessels could still be observed around the residual α-TCP particles (Figure 6 c). In the control group, α-TCP particles were surrounded by connective tissue, and new bone filled the bone defect; however, newly formed vessels were not observed overall (Figure 6 e, f). The thin new cementum formation with new PDLs in the control group was similar to that in the bFGF group (Figure 6 d).

At 8 weeks, new bone with a Haversian structure filled the entire bone defect in the bFGF group (Figure 7 b), and tissue specimens stained with Azan showed varied staining from dark blue to light purple in the newly formed bone (Figure 7 d). New vessels were particularly observed in the collagen fibers on the root surface (Figure 7 c). The dense fibers of connective tissue were arranged regularly, attaching the new bones and newly formed cementum (Figure 7 d). The height of the gingival tissue at was maintained at a high level and we did not observe ankylosis in the lesions between the root and the alveolar bone throughout the experimental period (Figure 7 b). In the control group, α-TCP particles persisted, although some were degraded (Figure 7 f), and some new vessels remained (Figure 7 g).

The ratio of new bone area to total area (BA/TA), new cementum (NC)/total height (TH) (%) and new PDL (NP)/total height (TA) (%) of each group was measured from the hematoxylin and eosin-stained sections (Figure 8). The BA/TA ratio of the bFGF group was significantly higher than that of the control group at each time point examined ($p < 0.05$). The ratio of NC/TH and NP/TA of the bFGF

group was significantly higher than those of control group at 4 weeks ($p < 0.05$). The ratio of NC/TH and NP/TA in the control group was not determined at 2 weeks (Figure 8).

Discussion

bFGF-2 is a heparin−binding growth factor that exhibits potent angiogenic and mitogenic ability in mesenchymal cells [15,16]. In addition, bFGF-2 enhances the formation of new alveolar bone, cementum, and PDL [17]. In this study, we immobilized bFGF on porous α-TCP particles, using heparin. The modified α-TCP particles were then implanted into canine mandibular 2-wall periodontal defects, and the regenerated periodontium was evaluated for up to 8 weeks.

Canines are suitable models for monitoring bone regeneration during correction of mandibular defects because the sizes and types of deformations that can be created in these animals approximate those seen in human patients [18]. Large periodontal defects in canines featuring significant destruction of periodontal tissue are difficult to heal after periodontal surgery, and one-wall intrabony defects are recognized as defects of this type [19,20]. Previously, Anzai et al. [21] investigated the long-term stability and qualitative equivalence of the periodontal tissues after FGF-2 treatment in a Beagle dog model of 2-wall periodontal defects. In the present study, we created 2-wall intrabony defects to prevent leakage of the α-TCP particles.

The optimal dose of bFGF depends on the carrier used. In our previous study [9], the amount of immobilized bFGF was quantified using ^{125}I-labeled bFGF; we determined that 59.6 ± 3.1 ng of bFGF could be immobilized on 1 mg of α-TCP particles. In the present study, the mandibular defects were filled with approximately 100 mg of porous α-TCP particles, corresponding to a total of approximately 5.9 μg of bFGF. Previously, Sato et al. [22] used 1 μg of bFGF and demonstrated the formation of dense fibers bound to the alveolar bone and newly synthesized cementum in the teeth of a beagle dog model. Addin et al. [23] demonstrated that gelatin/β-TCP sponges containing 30 μg of recombinant human FGF-2 (rhFGF-2) showed an increased potential to support periodontal wound healing and regeneration in canine recession-type defects.

Micro-CT has a high resolution and requires very thin specimen slices. With a larger number of slices, the spatial differences within areas of the specimen become negligible [24]. The geometrical properties of the healing bone can be acquired along with the spatial distribution of BMD through simultaneous scans of a calibration phantom using micro-CT [24]. In the 3D analysis, VD and BMC were measured directly, whereas BMD was calculated from the BV and BMC. In our study, VD and BMD were higher at all time points in the bFGF group than in the control group; however, the difference was not significant. By contrast, BMC was significantly higher in the bFGF group than in the control group at 2 and 4 weeks post-transplant. The bone quality determined from BMC of the experimental group was also considerably better than that of the control group. These results suggest that porous bFGF promoted new bone formation in the early stages. The pattern of changes in the BMD, BMC, and VD obtained by 3D analysis was different from that of BA/TA obtained by histological assessment. The reason is unclear, however, the residual αTCP particles might have been recognized as new bone in the 3D analysis. On the other hand, the identification of the between residual αTCP particles and new bone was easy in the histological assessment.

In the bFGF group, new bone formation and vascularization around the porous α-TCP particles was observed by histological examination at 2 weeks post-surgery, which is consistent with our previous study [9] that utilized porous α-TCP with immobilized bFGF in a canine four-wall bone defect model. In another study, bFGF was reported to induce the proliferation of osteoblasts and periosteal cells *in vitro* [25], and to stimulate bone formation during the early stages of cranial bone regeneration in a murine model [26]. Together, these findings indicate that the presence of bFGF at the defect site is essential to induce new bone formation and to provide sufficient blood flow to the regenerated bone tissue in the early stages of healing. In addition, the porous structure of the α-TCP particles might stimulate capillary action and show high affinity for blood from the original bone. It has been reported that calcium phosphate blockade does not lead to the formation of new blood vessels, which is crucial for bone formation, and that a porous structure is necessary to increase blood vessel formation and to harbor progenitor cells and signaling factors [5,27]. We frequently observed ingrowth of blood vessel-like structures in the scaffold containing bFGF2 compared with that in the control

group in the present study; thus, we speculated that the effect of bFGF2 on blood vessel formation is important for bone tissue remodeling.

Furthermore, the early formation of connective tissue induced by bFGF-2 maintained the height of the gingival tissue, thus creating a regenerative space and eventually promoting the regeneration of new cementum and PDL on the root surface. Previously, Efthimia et al. [28] showed that human PDL fibroblasts exhibit *in vitro* phenotypic characteristics that are consistent with osteoblast-like cells and that such cells have the potential to differentiate into osteoblasts and cementoblasts. During the early stages of periodontal tissue regeneration, bFGF-2 increased the number of fibroblastic cells, including mesenchymal stem cells, and promoted angiogenesis. During the subsequent healing processes, when the bFGF immobilized on the α-TCP particles appeared gradually at the administration site, the fibroblastic cells might have begun to differentiate into osteoblasts, cementoblasts, and PDL cells, thus inducing marked periodontal tissue regeneration.

Conclusion

In summary, we evaluated the effects of bFGF immobilized on porous α-TCP particles on periodontal wound healing, using a canine mandibular 2-wall periodontal defect model. Healing of the alveolar bone and periodontal attachment was strongly promoted by modified α-TCP implantation. In addition, the modified α-TCP scaffold consistently suppressed aberrant healing processes, such as ankylosis and root resorption. One important factor to note is that we used a surgically created model of a periodontal defect, which might show higher healing potential than a clinically encountered defect. Therefore, similar experiments need to be conducted in the clinical setting to verify the results. Nevertheless, our results indicate that bFGF immobilized on α-TCP particles could effectively reduce the time required to regenerate the periodontium, thus highlighting the potential of porous α-TCP particles with immobilized bFGF for use in regeneration of the periodontal tissue.

Acknowledgments

This work was funded by a MEXT/Japan Society for the Promotion of Science KAKENHI grant (No. 25463062), by the Japan Agency for Medical Research and Development (No. 17ek0109138h0003), and by Osaka Dental University Research Funds (17-10).
.

Conflicts of Interest

The authors declare no conflicts of interest.

References

1. Matsuno T, Nakamura T, Kuremoto K, Notazawa S, Nakahara T, Hashimoto Y, Satoh T, Shimizu Y (2006) Development of beta-tricalcium phosphate/collagen sponge composite for bone regeneration. Dent Mater J 25:138-144
2. Omata K, Matsuno T, Asano K, Hashimoto Y, Tabata Y, Satoh T (2014) Enhanced bone regeneration by gelatin-β-tricalcium phosphate composites enabling controlled release of bFGF. J Tissue Eng Regen Med 8:604-611
3. Baba S, Inoue T, Hashimoto Y, Kimura D, Ueda M, Sakai K, Matsumoto N, Hiwa C, Adachi T, Hojo M (2010) Effectiveness of scaffolds with pre-seeded mesenchymal stem cells in bone regeneration - Assessment of osteogenic ability of scaffolds implanted under the periosteum of the cranial bone of rats. Dent Mater J 29:673-681
4. Hammarström L, Heijl L, Gestrelius S (1997) Periodontal regeneration in a buccal dehiscence model in monkeys after application of enamel matrix proteins. J Clin Periodontol 24:669-677
5. Sakai K, Hashimoto Y, Baba S, Nishiura A, Matsumoto N (2011) Effects on bone regeneration when collagen model polypeptides are combined with various sizes of alpha-tricalcium phosphate particles. Dent Mater J 30:913-922
6. Kitamura M, Ohtsuki C, Iwasaki H, Ogata SI, Tanihara M, Miyazaki T (2004) The controlled resorption of porous α-tricalcium phosphate using a hydroxypropylcellulose coating. J Mater Sci Mater Med 15:1153-1158
7. Tabata Y, Yamada K, Miyamoto S, Nagata I, Kikuchi H, Aoyama I, Tamura M, Ikada Y (1998) Bone regeneration by basic fibroblast growth factor complexed with biodegradable hydrogels. Biomaterials 19:807-815
8. Kakinoki S, Sakai Y, Fujisato T, Yamaoka T (2015) Accelerated tissue integration into porous materials by immobilizing basic fibroblast growth factor using a biologically safe three‐step

reaction. J Biomed Mater Res A 103:3790-3797

9. Kobayashi N, Hashimoto Y, Otaka A, Yamaoka T, Morita S (2016) Porous Alpha-Tricalcium Phosphate with Immobilized Basic Fibroblast Growth Factor Enhances Bone Regeneration in a Canine Mandibular Bone Defect Model. Materials 9:853

10. Saito E, Saito A, Kato H, Shibukawa Y, Inoue S, Yuge F, Nakajima T, Takahashi T, Kawanami M (2016) A novel regenerative technique combining bone morphogenetic protein-2 with fibroblast growth factor-2 for circumferential defects in dog incisors. J Periodontol 87:1067-1074

11. Sigurdsson TJ, Nygaard L, Tatakis DN, Fu E, Turek TJ, Jin L, Wozney JM, Wikesjö UME (1996) Periodontal Repair in Dogs: Evaluation of rhBMP-2 Carriers. Int J Periodontics Restorative Dent 16:525-537

12. Sorensen RG, Wikesjö UME, Kinoshita A, Wozney JM (2004) Periodontal repair in dogs: Evaluation of a bioresorbable calcium phosphate cement (Ceredex™) as a carrier for rhBMP-2. J Clin Periodontol 31:796-804

13. Wikesjö UME, Guglielmoni P, Promsudthi A, Cho KS, Trombelli L, Selvig KA, Jin L, Wozney JM (1999) Periodontal repair in dogs: Effect of rhBMP-2 concentration on regeneration of alveolar bone and periodontal attachment. J Clin Periodontol 26:392-400

14. Young C, Ladd P, Browning C, Thompson A, Bonomo J, Shockley K, Hart C (2009) Release, biological potency, and biochemical integrity of recombinant human platelet-derived growth factor-BB (rhPDGF-BB) combined with Augment TM bone graft or GEM 21S beta-tricalcium phosphate (β-TCP). J Control Release 140:250-255

15. Kotev-Emeth S, Savion N, Pri-chen S, Pitaru S (2000) Effect of maturation on the osteogenic response of cultured stromal bone marrow cells to basic fibroblast growth factor. Bone 27:777-783

16. Moscatelli D, Joseph-Silverstein J, Presta M, Rifkin DB (1988) Multiple forms of an

angiogenesis factor: basic fibroblast growth factor. Biochimie 70:83-87

17. Kitamura M, Nakashima K, Kowashi Y, Fujii T, Shimauchi H, Sasano T, Furuuchi T, Fukuda M, Noguchi T, Shibutani T (2008) Periodontal tissue regeneration using fibroblast growth factor-2: randomized controlled phase II clinical trial. PLoS One 3:e2611

18. Carrel JP, Wiskott A, Scherrer S, Durual S (2016) Large Bone Vertical Augmentation Using a Three‐Dimensional Printed TCP/HA Bone Graft: A Pilot Study in Dog Mandible. Clin Implant Dent Relat Res

19. Lee JS, Wikesjö UM, Jung UW, Choi SH, Pippig S, Siedler M, Kim CK (2010) Periodontal wound healing/regeneration following implantation of recombinant human growth/differentiation factor‐5 in a β‐tricalcium phosphate carrier into one‐wall intrabony defects in dogs. J Clin Periodontol 37:382-389

20. Matsuura T, Akizuki T, Hoshi S, Ikawa T, Kinoshita A, Sunaga M, Oda S, Kuboki Y, Izumi Y (2015) Effect of a tunnel‐structured β‐tricalcium phosphate graft material on periodontal regeneration: a pilot study in a canine one‐wall intrabony defect model. J Periodontal Res 50:347-355

21. Anzai J, Nagayasu-Tanaka T, Terashima A, Asano T, Yamada S, Nozaki T, Kitamura M, Murakami S (2016) Long-term Observation of Regenerated Periodontium Induced by FGF-2 in the Beagle Dog 2-Wall Periodontal Defect Model. PLoS One 11:e0158485

22. Sato Y, Kikuchi M, Ohata N, Tamura M, Kuboki Y (2004) Enhanced cementum formation in experimentally induced cementum defects of the root surface with the application of recombinant basic fibroblast growth factor in collagen gel in vivo. J Periodontol 75:243-248

23. Shujaa Addin A, Akizuki T, Hoshi S, Matsuura T, Ikawa T, Fukuba S, Matsui M, Tabata Y, Izumi Y (2017) Biodegradable gelatin/beta‐tricalcium phosphate sponges incorporating recombinant human fibroblast growth factor‐2 for treatment of recession‐type defects: A split‐mouth study in dogs. J Periodontal Res

24. Tobita K, Ohnishi I, Matsumoto T, Ohashi S, Bessho M, Kaneko M, Matsuyama J, Nakamura K (2011) Effect of low-intensity pulsed ultrasound stimulation on callus remodelling in a gap-healing model Evalustion by bone morphemetry using three-dimeentional quantitative micro-CT. J Bone Joint Surg 93:525-530

25. Pri-Chen S, Pitaru S, Lokiec F, Savion N (1998) Basic fibroblast growth factor enhances the growth and expression of the osteogenic phenotype of dexamethasone-treated human bone marrow-derived bone-like cells in culture. Bone 23:111-117

26. Shimizu A, Tajima S, Tobita M, Tanaka R, Tabata Y, Mizuno H (2014) Effect of control-released basic fibroblast growth factor incorporated in β-tricalcium phosphate for murine cranial model. Plast Reconstr Surg 2:e126

27. Ito T, Hashimoto Y, Baba S, Iseki T, Morita S (2015) Bone Regeneration With a Collagen Model Polypeptides/α-Tricalcium Phosphate Sponge in a Canine Tibia Defect Model. Implant Dent 24:197-203

28. Basdra EK, Komposch G (1997) Osteoblast-like properties of human periodontal ligament cells: an in vitro analysis. Eur J Orthod 19:615-621

Figure Captions

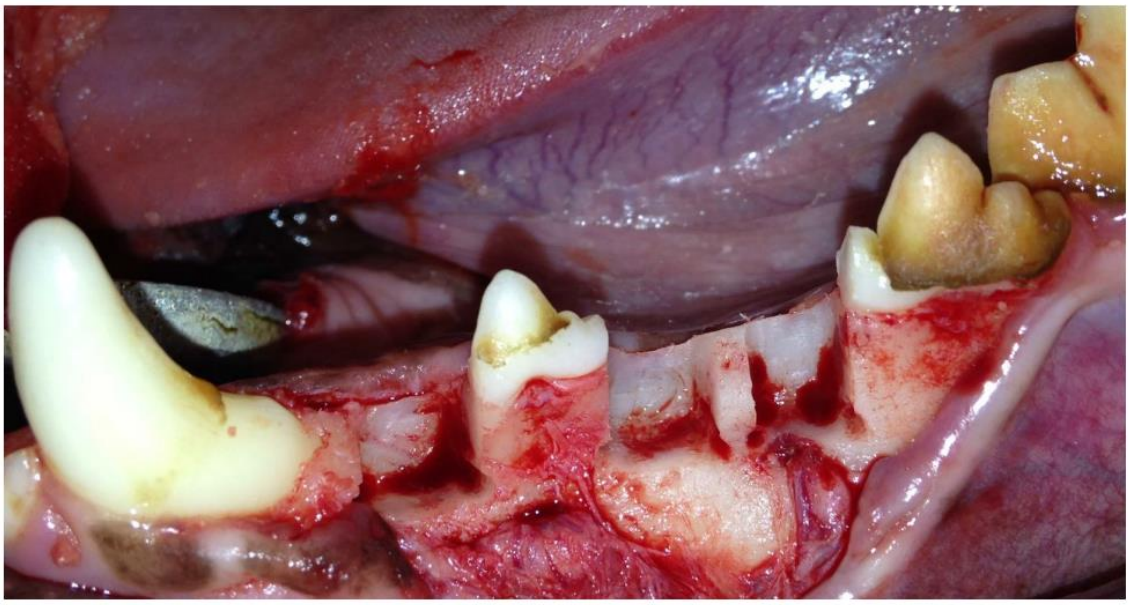

Fig. 1 Photographs of the surgically created 2-wall periodontal defect

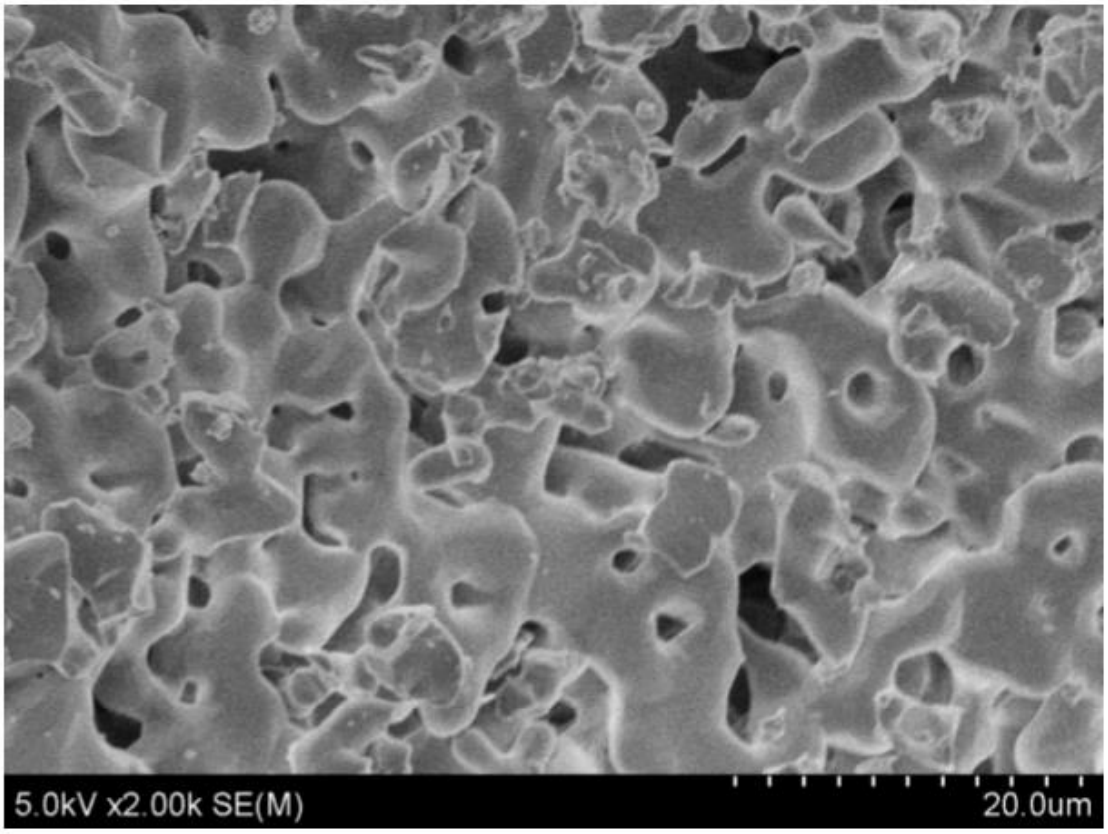

Fig. 2 Scanning electron micrographs of alpha-tricalcium phosphate (α-TCP) particles

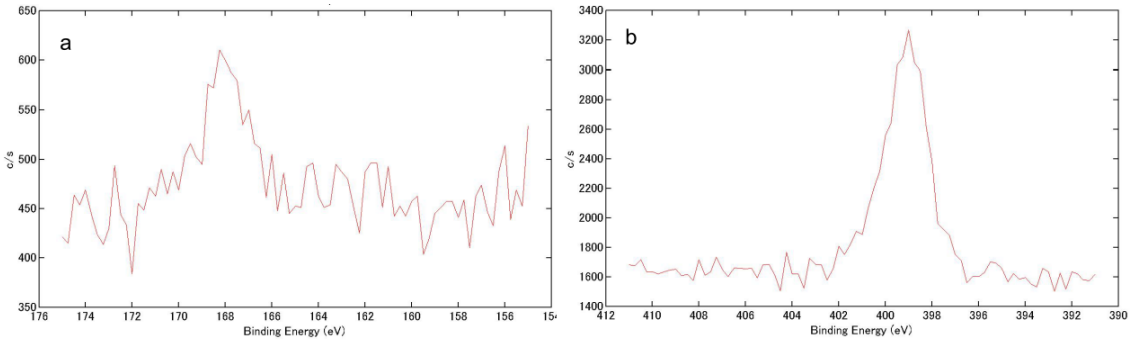

Fig. 3 Surface characterization of basic fibroblast growth factor (bFGF) bound to porous alpha-tricalcium phosphate (α-TCP) particles via heparin. (a) X-ray photoelectron spectroscopy (XPS) S 2p and (b) XPS N 1s spectra

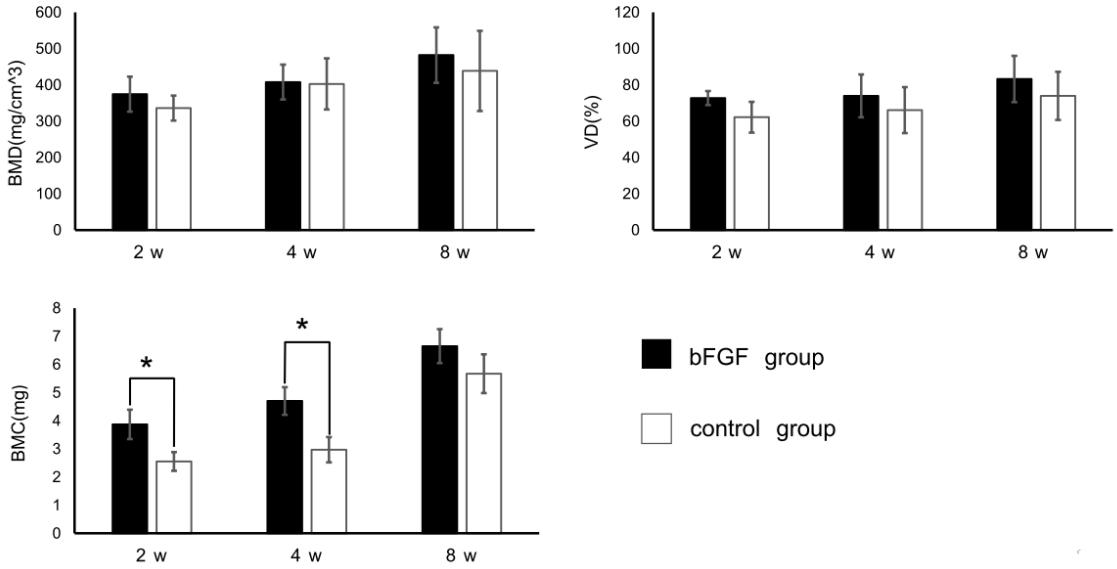

Fig. 4 Bone mineral density (BMD), volumetric density (VD), and bone mineral content (BMC) in the basic fibroblast growth factor (bFGF) and control groups at 2, 4, and 8 weeks. * $p < 0.05$

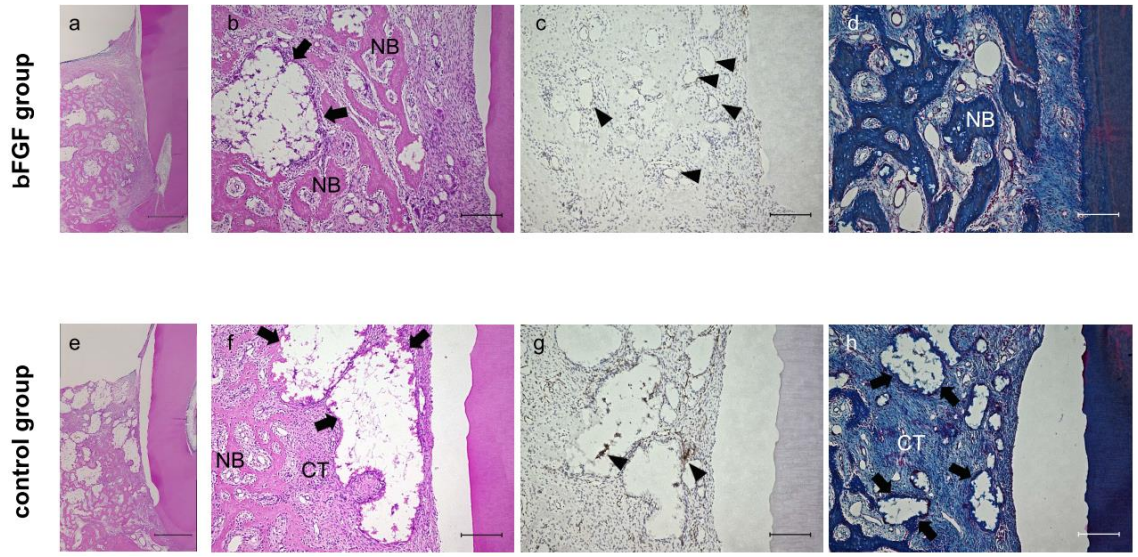

Fig. 5 Hematoxylin and eosin (H&E)-stained sections (a, b, e, f), immunostaining (c, g), and Azan staining (d, h) of bone defects in the basic fibroblast growth factor (bFGF) (a, b, c, d) and control (e, f, g, h) groups at 2 weeks.

CT, connective tissue; NB, newly formed bone; black triangles, new vessels labeled for von Willebrand Factor (vWF); black arrows, residual granules; NC, new cementum; PL, periodontal ligament. bars a, e = 1000 μm, others = 200 μm

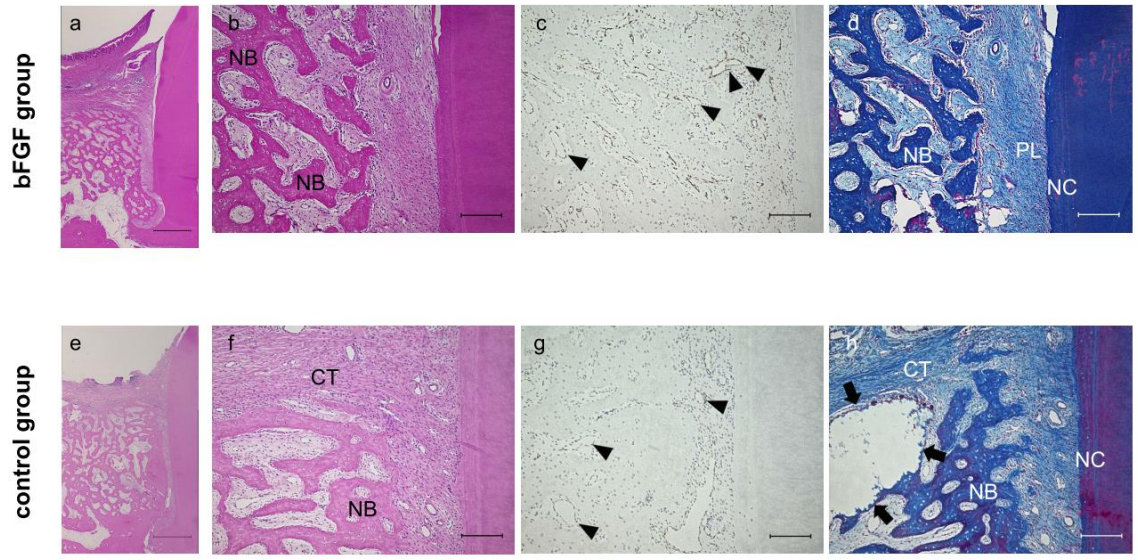

Fig. 6 Hematoxylin and eosin (H&E)-stained sections (a, b, e, f), immunostaining (c, g), and Azan staining (d, h) of bone defects in the basic fibroblast growth factor (bFGF) (a, b, c, d) and control (e, f, g, h) groups at 4 weeks

CT, connective tissue; NB, newly formed bone; black triangles, new vessels labeled for von Willebrand Factor (vWF); black arrows, residual granule; NC, new cementum; PL, periodontal ligament. Bars a, e = 1000 μm, others = 200 μm

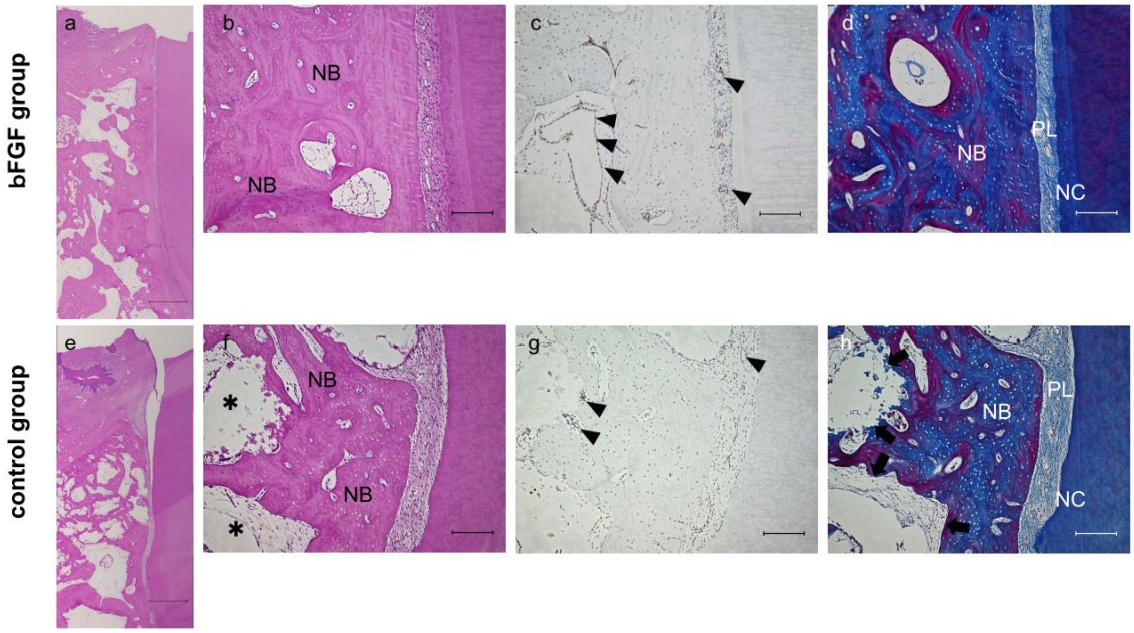

Fig. 7 Hematoxylin and eosin (H&E)-stained sections (a, b, e, f), immunostaining (c, g), and Azan staining (d, h) of bone defects in the basic fibroblast growth factor (bFGF) (a, b, c, d) and control (e, f, g, h) groups at 8 weeks

CT, connective tissue; NB, newly formed bone; black triangles, new vessels labeled for von Willebrand Factor (vWF); black arrows, residual granule; NC, new cementum; PL, periodontal ligament. Bars a, e =1000 μm, others=200 μm

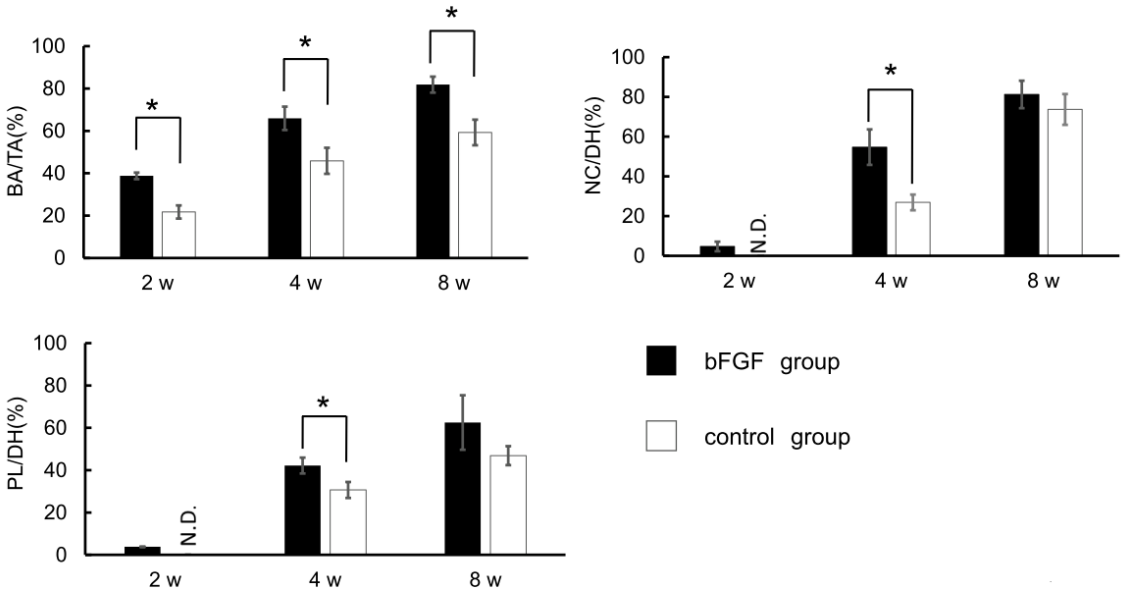

Fig. 8 New bone, cementum, and periodontal ligaments (PDL) formation was quantified by determining the new bone area (BA)/total defect area (TA) (%), new cementum (NC)/total height (TH) (%), and new PDL (NP)/total height (TA) (%) from the hematoxylin and eosin (H&E)-stained sections. * $p < 0.05$